

# Break-up fragments excitation and the freeze-out volume

Ad. R. Raduta<sup>1,2</sup>, E. Bonnet<sup>1</sup>, B. Borderie<sup>1</sup>, N. Le Neindre<sup>1</sup> and M. F. Rivet<sup>1</sup>

<sup>1</sup>*Institut de Physique Nucléaire, IN2P3-CNRS, F-91406 Orsay cedex, France*

<sup>2</sup>*NIPNE, Bucharest-Magurele, POB-MG 6, Romania*

## Abstract

We investigate, in microcanonical multifragmentation models, the influence of the amount of energy dissipated in break-up fragments excitation on freeze-out volume determination. Assuming a limiting temperature decreasing with nuclear mass, we obtain for the Xe+Sn at 32 MeV/nucleon reaction [J. D. Frankland *et al.*, Nucl. Phys. A689, 905 (2001); A689, 940 (2001)] a freeze-out volume almost half the one deduced using a constant limiting temperature.

PACS numbers: 25.70.Pq Multifragment emission and correlations, 24.10.Pa Thermal and statistical models

## I. INTRODUCTION

One on the most provocative objectives of nowadays nuclear physics, the determination of the phase diagram of excited nuclear systems, requires precise measurements of relevant thermodynamical observables, volume and temperature.

From the theoretical point of view, the freeze-out volume is regarded as an external constraint as in microcanonical multifragmentation models [1, 2, 3, 4] or simply as the volume in which are situated the non-interacting fragments as in dynamical models [5]. From the experimental point of view, the estimation of the freeze-out volume is delicate since break-up information is altered by secondary particle emission and non-equilibrium phenomena. The difficulty of determining the freeze-out volume is reflected in the different values obtained by theoretical models [1, 2, 6, 7, 8] and particle interferometry experiments [9] which range from  $2.5V_0$  to  $9V_0$ , where  $V_0$  is the volume corresponding to normal nuclear matter density.

The aim of the present study is to investigate to what extent the freeze-out volume obtained by microcanonical multifragmentation models depends on the definition of break-up fragments in terms of excitation energy. Section II makes a review on how the observables characterizing the equilibrated state of the system are determined by microcanonical multifragmentation models. Section III presents the evolution of statistical and kinetic fragment distributions of a given system when one modifies the amount of energy dissipated as excitation energy of primary fragments. Section IV presents the dramatic reduction of the freeze-out volume when a mass-dependent limiting temperature is employed. The conclusions are formulated in Section V.

## II. FRAGMENT FORMATION IN MICROCANONICAL MODELS

Microcanonical models for multifragmentation describe the fragment partition of the equilibrated source ( $A, Z, E_{ex}, \mathbf{L}, V$ ) taking into account all configurations that are geometrically possible and are not forbidden by conservation laws. Thus, the available energy of the system ( $E_{ex}$ ) is used up in fragment formation ( $Q$ ), internal excitation ( $\sum_i \epsilon_i$ ), fragment-fragment Coulomb interaction ( $\sum_{i < j} V_{ij}$ ) and thermal motion  $K$ ,

$$K = E_{ex} - Q - \sum_i \epsilon_i - \sum_{i < j} V_{ij}, \quad (1)$$

and determines together with fragments internal state the statistical weight of any configuration [4],

$$W_C \propto \frac{1}{N_C!} \prod_{n=1}^{N_C} \left( \Omega \frac{\rho_n(\epsilon_n)}{h^3} (mA_n)^{3/2} \right) \cdot \frac{2\pi}{\Gamma(3/2(N_C - 2))} \cdot \frac{1}{\sqrt{(\det I)}} \cdot \frac{(2\pi K)^{3/2N_C - 4}}{(mA)^{3/2}}. \quad (2)$$

From Eq. 1 it is obvious that there is a strong interplay between all energetic degrees of freedom. While the Q-value depends exclusively on fragment partition, the Coulomb energy depends on both fragment partition and volume. The excitation energy absorbed by fragments is determined by the maximum allowed excitation and level density. As fragments definition at break-up depends on the underlying break-up scenario, it is postulated by each model. Thus, MMMC [1] considers primary fragments rather cold which decay mainly by neutron evaporation. On the other hand, SMM [2] allows fragments to excite to much higher energies but their internal temperature is fixed by the translational one, as authors expect to happen when thermodynamical equilibrium is achieved. Finally, MMM [4] assumes the fragment binding energy as the upper limit for internal excitation. Obviously, more excited the break-up fragments are, more abundant is the secondary particle emission. Recent experimental data [10] based on relative velocity correlations between light charged particles and fragments provide for the excitation energy of primary fragments obtained in central collisions of Xe+Sn from 32 to 50 MeV/nucleon values around 2-3 MeV/nucleon confirming the hypotheses of hot primary fragments.

The established method to identify the equilibrated source corresponding to a given experimental multifragmentation reaction is to tune the values of the source parameters such as to describe as well as possible all available statistical and kinetic fragment distributions.

Even if the conclusions of the present study hold for all versions of the microcanonical multifragmentation model we shall use the MMM version [4, 8] to illustrate them. In particular, we shall focus on the case of the Xe+Sn at 32 MeV/nucleon multifragmentation reaction [11] because it offers one of the most complete set of experimental data in the literature and made the object of a rather comprehensive investigation on source identification using MMM [8].

Thus, employing the level density formula,

$$\rho(\epsilon) = \frac{\sqrt{\pi}}{12a^{1/4}\epsilon^{5/4}} \cdot \exp(2\sqrt{a\epsilon}) \cdot \exp(-\epsilon/\tau), \quad (3)$$

with  $a = 0.114A + 0.098A^{2/3}$  MeV $^{-1}$  [12] and  $\tau=9$  MeV, Ref. [8] reached the conclusion that the freeze-out volume is 8 - 9  $V_0$ .

To test the excitation energy effect of freeze-out volume identification, we hold the fragments binding energy as the upper limit of their excitation and modify the amount of energy dissipated in internal excitation by varying the limiting temperature  $\tau$ . Three values will be considered in our study:  $\tau=9$  MeV as in Ref. [8], an arbitrarily chosen smaller value, 5 MeV and a mass dependent limiting temperature,  $\tau(A) = 4.3 + 18.3/\sqrt{A} - 19.9/A$  MeV. The decrease of the limiting temperature with the fragment mass was demonstrated by phenomenological analyses of the evolution of the caloric curve plateau temperature and mean field calculations [13, 14]. The considered expression of  $\tau(A)$  was obtained from a fit over data presented in Refs. [13] and [14] and ranges between the two above considered values ( $\tau(A = 5) = 8.5$  MeV and  $\tau(A = 200) = 5.5$  MeV).

### III. EFFECT OF FRAGMENT EXCITATION ON FRAGMENT DISTRIBUTIONS

Fig. 1 depicts the break-up stage charge distributions obtained from the multifragmentation of the (230, 94) nuclear system with  $E_{ex}=5.3$  MeV/nucleon and  $V = 9V_0$ . This is the source for which, assuming the break-up fragments as hard non-overlapping spheres localized in a spherical container (the freeze-out volume), MMM obtained the best agreement with the experimental data corresponding to Xe+Sn at 32 MeV/nucleon [8]. As one may see, in this particular situation, the effect of diminishing the limiting temperature from 9 to 5 MeV is very small,  $Y(Z)$  corresponding to lower excitation energies being barely steeper thus indicating a more advanced fragmentation. Indeed, following the evolution of average partial energies summarized in Table I, it results that the decrease of average total excitation energy leads to an increase of almost 50% of the Q-value. However, the total number of fragments increases by only 18% such that the average total Coulomb field (which is maximum when the freeze-out volume is populated uniformly) increases very little. The energy excess is transformed into thermal motion.

Much more exciting is the situation when the constant  $\tau$  is replaced with the mass-dependent one. As the produced fragments have  $Z$  smaller than 60,  $\tau$  ranges between 6.3 and 8.5 MeV and the excitation energy is lower than the one obtained for  $\tau=9$  MeV and higher than the one corresponding to  $\tau=5$  MeV, as confirmed by the values in Table I and average excitation energy per nucleon of primary fragments represented in Fig. 2 as a function of fragment charge. As expected, the evolution of average total excitation energy is reflected in the evolution of average

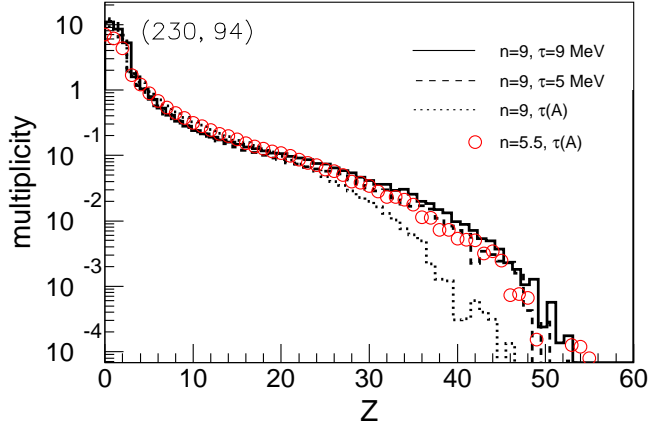


FIG. 1: Break-up charge distributions corresponding to the (230, 94) nuclear system with  $E_{ex}=5.3$  MeV/nucleon and  $9V_0$  (solid, dashed and dotted lines) and  $5.5V_0$  (open circles). The amount of excitation energy absorbed by primary fragments is modified via the limiting temperature,  $\tau$ .

TABLE I: Break-up stage values of average total Coulomb energy, thermal kinetic energy,  $Q$ -value, excitation energy expressed in MeV and total multiplicity (including neutrons and light charged particles) obtained in the multifragmentation of (230, 94) nuclear system with  $E_{ex}=5.3$  MeV/nucleon and different freeze-out volumes and excitation of primary fragments, as indicated in the first column.

$(V/V_0, \tau)$	$V_{Coulomb}$	$K_{thermal}$	$Q$	$\epsilon_{tot}$	Total multiplicity
(9, 9)	390.61	287.67	186.59	354.13	32.5
(9, 5)	406.96	347.29	270.86	193.89	38.4
(9, $\tau(A)$ )	413.33	294.01	232.56	279.10	34.0
(5.5, $\tau(A)$ )	473.17	257.63	145.37	342.83	26.2

excitation of each emitted fragment. A more interesting remark is that, as far as the limiting temperature is constant, the average excitation energy per nucleon increases slowly with fragment size reflecting the increase of the binding energy over the considered mass domain, while a mass decreasing  $\tau$  produces an opposite behavior. Moreover, the steep increase of the binding energies for small fragments corroborated with the decreasing  $\tau$  induces a hump in the fragment excitation energy distributions. It is worthwhile to mention here that the distribution corresponding to  $\tau=9$

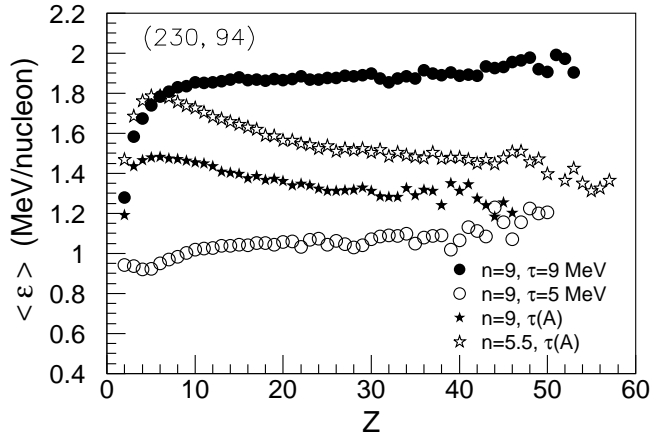


FIG. 2: Average excitation energies of primary fragments obtained from the multifragmentation of the (230,94) nuclear system with  $E_{ex}=5.3$  MeV/nucleon and different freeze-out volumes and limiting temperatures.

MeV is in acceptable agreement with the experimentally deduced one [10].

An intermediate value of excitation energy induces an intermediate Q-value and, not obvious, a strong narrowing of the  $Y(Z)$  distributions. The effect on fragment partitions can be understood analyzing the statistical weight of a configuration. The ratio between a partition with  $N$  fragments  $\{A_1, A_2, \dots, A_i, \dots, A_N\}$  and the partition in which the  $i$ -th fragment is replaced by two smaller fragments  $i'$  and  $j'$  ( $A_{i'} + A_{j'} = A_i$ ) is,

$$\frac{W_{C_N}}{W_{C_{N+1}}} \propto \frac{\rho(\epsilon_i)}{\rho(\epsilon_{i'})\rho(\epsilon_{j'})} = \left( \frac{a_{i'}a_{j'}}{a_i} \right)^{1/4} \cdot \left( \frac{\epsilon_{i'}\epsilon_{j'}}{\epsilon_i} \right)^{5/4} \cdot \frac{12}{\sqrt{\pi}} \cdot \exp \left( 2\sqrt{a_i\epsilon_i} - 2\sqrt{a_{i'}\epsilon_{i'}} - 2\sqrt{a_{j'}\epsilon_{j'}} \right) \cdot \exp \left( -\frac{\epsilon_i}{\tau_i} + \frac{\epsilon_{i'}}{\tau_{i'}} + \frac{\epsilon_{j'}}{\tau_{j'}} \right). \quad (4)$$

To simplify the estimation one can consider that for the large fragments ( $Z > 20$ ) the excitation energy per mass number is constant,  $\epsilon = \langle \epsilon \rangle \cdot A$ . If  $\tau$  is constant, the factor  $\exp \left( -\frac{\epsilon_i}{\tau_i} + \frac{\epsilon_{i'}}{\tau_{i'}} + \frac{\epsilon_{j'}}{\tau_{j'}} \right)$  vanishes and the expression in Eq. 4 has no explicit dependence on  $\tau$ . In this case, the fragment partitions are selected by the other factors entering the statistical weight formula, including those which depend on the internal excitation ( $\epsilon^{5/4} \cdot \exp(2\sqrt{A\epsilon})$ ). If  $\tau$  is decreasing with  $A$ , the last factor in Eq. 4 is smaller than 1, meaning that configurations with smaller fragments will be favored, as reflected by the  $Y(Z)$  distributions (see Fig. 1).

Because an additional key quantity to determine the freeze-out volume is the fragment average kinetic energy distribution as a function of charge, in Fig. 3 are presented the break-up and

asymptotic stage results for the above discussed situations. To maintain the comparison with the Xe+Sn at 32 MeV/nucleon case straightforward, we considered for all cases the collective energy equal to 1.4 MeV/nucleon as in Ref. [8]. While the increase of both Coulomb and thermal energy obtained when  $\tau=9$  MeV is replaced with 5 MeV would seem to produce higher  $\langle K \rangle$  versus  $Z$  distributions, the upper panel of Fig. 3 shows the opposite. This effect is due to an even stronger increase of the total number of emitted fragments which automatically results in smaller kinetic energy per fragment [15]. Concerning the evolution from  $\tau=5$  MeV to  $\tau(A)$ ,  $\langle K \rangle$  versus  $Z$  is slightly affected meaning that partial energy and total number of fragments modifications compensate each other.

Because the experimentally detected fragments are the asymptotic ones, the lower panel of Fig. 3 depicts the asymptotic  $\langle K \rangle$  versus  $Z$  distributions. More excited the fragments are, stronger will be the effect of particle evaporation. Thus, despite the average kinetic energies of intermediate size fragments obtained for  $\tau=9$  MeV is 10 MeV larger than the ones corresponding to  $\tau=5$  MeV, after sequential evaporation they overlap.

To recover the initial fragment yield distribution with a  $\tau(A)$  dependence, one has to diminish the freeze-out volume. In Figs. 1 and 3 are represented with open circles the corresponding distributions obtained for the same value of  $E_{ex}=5.3$  MeV/nucleon. As indicated in the figure,  $Y(Z)$  gets its initial shape for  $V = 5.5V_0$ . Such a small freeze-out volume results in a stronger Coulomb field (Table I) moving upward the  $\langle K \rangle(Z)$  distribution. This suggests that in this case the description of the experimental data will require a smaller amount of flow.

#### IV. APPLICATION ON EXPERIMENTAL DATA

To illustrate quantitatively the impact of assuming lower fragment excitation energies on freeze-out volume determination we choose the most spectacular situation of a mass dependent  $\tau$ . To characterize the complete state of the fused system we adopt the procedure used in Ref. [8] and the same Xe+Sn at 32 MeV/nucleon reaction. The freeze-out volume and source excitation are mainly determined by fitting the  $Y(Z)$  distribution, while the source size and excitation are fixed by the bound charge multiplicity and multiplicity of intermediate mass fragments. The amount of flow and the flow profile  $\alpha$  are tuned such as to obtain a good agreement with the experimental average kinetic energy distribution as a function of charge. Thus, the newly identified source is:

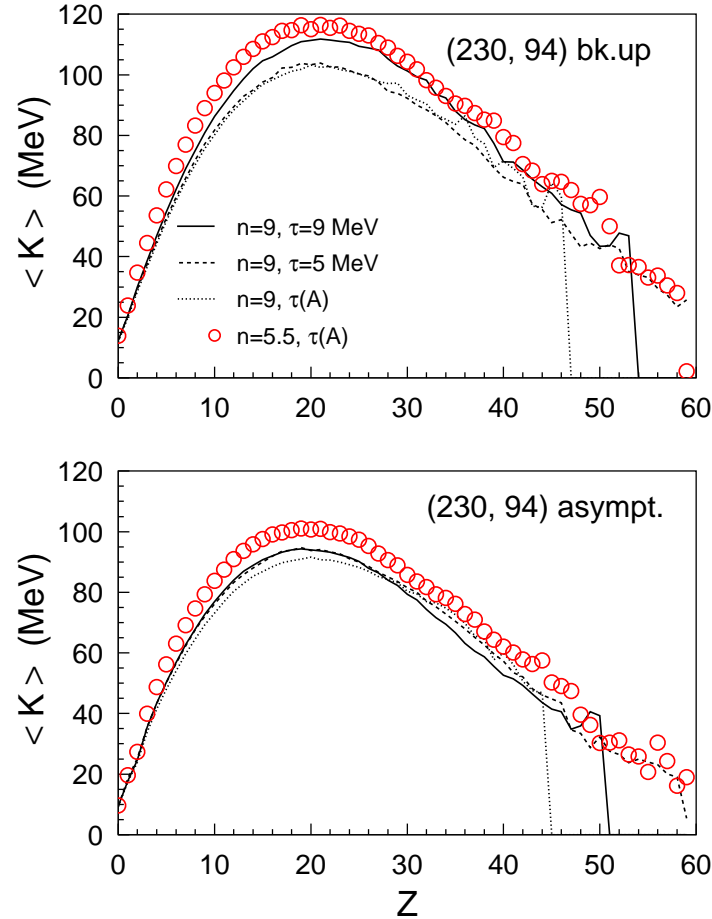


FIG. 3: Break-up stage (upper panel) and asymptotic stage (lower panel) mean kinetic energy distributions as a function of charge obtained for the above considered cases.

(220, 88),  $E_{ex}=5.1$  MeV/nucleon,  $V = 5V_0$ ,  $E_{flow}=1$  MeV/nucleon,  $\alpha = 1.8$ .

Figs. 4, 5 and 6 present the calculated asymptotic stage charge multiplicity distribution, multiplicity of number of intermediate mass fragments ( $Z \geq 5$ ) and, respectively, average fragment kinetic energy as a function of charge in comparison with the experimental data.

The most striking result is the reduction of the freeze-out volume to about half of the previously determined value,  $9V_0$ . The modifications on mass and charge are minor (6%). The decrease of 30% of the added flow is a consequence of the stronger Coulomb field produced by the compressed matter for the same fragment partition.

The proposed set of observables is not expected to be necessarily the real one since the values depend dramatically on the assumed limiting temperature, but are perfect examples to illustrate

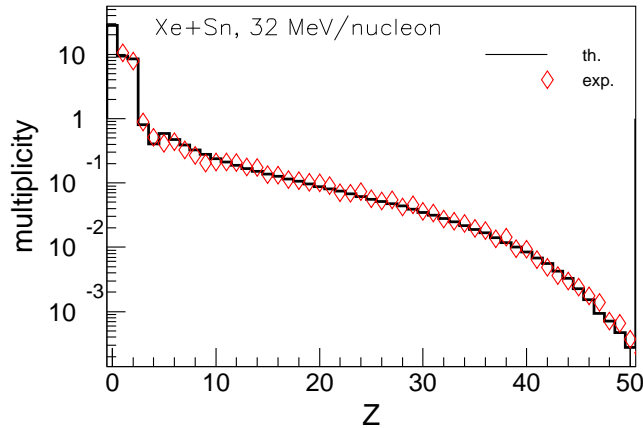


FIG. 4: Calculated asymptotic stage (histogram) and experimental (open symbols) charge distributions corresponding to Xe+Sn at 32 MeV/nucleon.

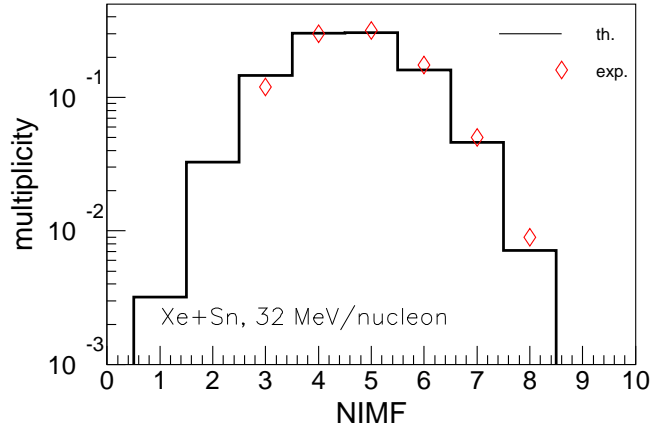


FIG. 5: Calculated asymptotic stage (histogram) and experimental (open symbols) distributions of multiplicity of number of intermediate mass fragments ( $Z \geq 5$ ) corresponding to Xe+Sn at 32 MeV/nucleon.

how break-up hypotheses dependent are the results obtained by statistical multifragmentation models.

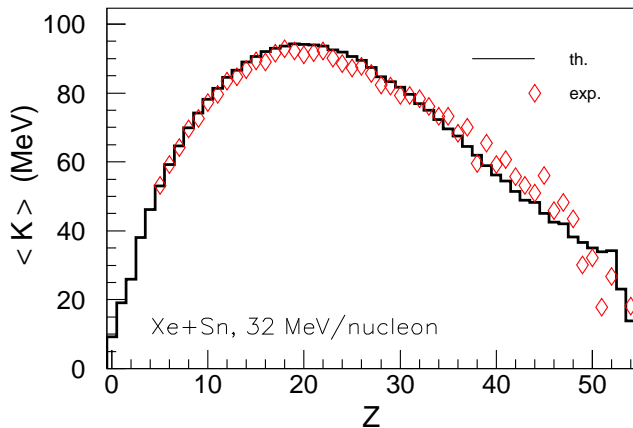


FIG. 6: Calculated asymptotic stage (histogram) and experimental (open symbols) distributions of fragment average kinetic energy as a function of charge corresponding to Xe+Sn at 32 MeV/nucleon.

## V. CONCLUSIONS

We investigate, in nuclear multifragmentation models, the sensitivity of freeze-out volume determination on primary fragment definition in terms of excitation energy. Assuming a mass dependent limiting temperature in concordance with recent phenomenological estimations and theoretical calculations, we distinguish a strong narrowing of charge distributions so that, to recover the agreement with a witness distribution, we have to assume a freeze-out volume almost half the one obtained with a constant limiting temperature.

Given the importance of accurate determination of the freeze-out volume, model-independent methods to measure this quantity and additional experimental information of the excitation state of primary fragments are necessary.

---

[1] D. H. E. Gross, Rep. Progr. Phys. **53**, 605 (1990).

[2] J. P. Bondorf, A. S. Botvina, A. S. Iljinov, I. N. Mishustin and K. Sneppen, Phys. Rep. **257**, 133 (1995).

[3] S. E. Koonin and J. Randrup, Nucl. Phys. A **474**, 173 (1987).

[4] Al. H. Raduta and Ad. R. Raduta, Phys. Rev. C **55**, 1344 (1997).

- [5] M. Parlog *et al.*, Eur. Phys. J. A **25**, 223 (2005).
- [6] Ph. Chomaz, M. Colonna, A. Guarnera and J. Randrup, Phys. Rev. Lett. **73**, 3512 (1994); A. Guarnera, Ph. Chomaz, M. Colonna and J. Randrup, Phys. Lett. **B403**, 191 (1997).
- [7] G. Tabacaru *et al.*, Nucl. Phys. A, in press.
- [8] Al. H. Raduta and Ad. R. Raduta, Phys. Rev. C **65**, 054610 (2002).
- [9] S. Fritz *et al.*, Phys. Lett. **B461**, 315 (1999).
- [10] S. Hudan *et al.*, Phys. Rev. C **67**, 064613 (2003).
- [11] J. D. Frankland *et al.*, Nucl. Phys. **A689**, 905 (2001); *ibid.* Nucl. Phys. **A689**, 940 (2001).
- [12] A. S. Iljinov, *et al.*, Nucl. Phys. **A543**, 517 (1992).
- [13] J. B. Natowitz, R. Wada, K. Hagel, T. Keutgen, M. Murray, A. Makeev, L. Qin, P. Smith, and C. Hamilton, Phys. Rev. C **65**, 034618 (2002) and references therein.
- [14] M. Baldo, L. S. Ferreira and O. E. Nicotra, Phys. Rev. C **69**, 034321 (2004).
- [15] Ad. R. Raduta, B. Borderie, E. Bonnet, N. Le Neindre, S. Piantelli and M. F. Rivet, Phys. Lett. **B623**, 43 (2005).